

102 Gbaud PAM-4 transmission over 2 km using a pulse shaping filter with asymmetric ISI and Tomlinson-Harashima Precoding

Xueyang Li, Zhenping Xing, Md Samiul Alam, Maxime Jacques, David V. Plant
 Department of Electrical and Computer Engineering, McGill University, Montréal, Québec, H3A 0E9, Canada
 Xueyang.li@mail.mcgill.ca

Abstract: We introduce the asymmetric-ISI pulse shaping filter with Tomlinson-Harashima precoding to increase the receiver RF swing, and demonstrate 102 Gbaud PAM-4 transmission over 2 km with a BER below 3.8×10^{-3} using linear equalizer at receiver. © 2020 The Author(s)

1. Introduction

Direct detection transceivers using 4-level pulse amplitude modulation (PAM-4) signaling are attractive for high throughput cost-sensitive intra data center interconnect, which has been adopted in the 400 GbE standard IEEE 802.3bs [1]. To scale to the next generation 800 GbE transceiver while maintaining the same form factor, single-lane 200 Gbit/s is required to save from adding additional wavelengths. This can be realized by either signaling at higher baud per wavelength or resorting to higher order modulation format beyond PAM-4, which requires more advanced digital-to-analog and analog-to-digital converters (DAC/ADC) with a higher effective number of bits (ENOB).

However, high baud signaling in a system composed of cost-effective but bandlimited electrical and optical components not only leads to strong inter symbol interference (ISI), but also weak RF swing at the receiver front-end, leading to degraded signal SNR due to the receiver noise. The postcursor ISI can be pre-compensated by Tomlinson Harashima precoding (THP), which is reported to realize up to 200 Gbit/s short reach IM/DD systems [2-4]. On the other hand, the weak RF swing at the receiver can be increased using our previously proposed controlled ISI pulse shaping [5], based on which 160 Gbit/s throughput per lane in a four-lane coarse wavelength division multiplexing (CWDM) system is demonstrated. However, the controlled ISI pulse shaping can only introduce symmetric ISI that is only partially mitigated by THP.

In this paper, we propose to increase the receiver RF swing in a 102 Baud IM/DD system by combining THP with a pulse shaping filter with asymmetric ISI, i.e. more dominant post-cursor ISI than pre-cursor ISI. The filter is obtained based on a cost-function that provides flexible tuning of the cost terms including the precursor and postcursor ISI such that we can best trade off the performance-related filter parameters. Since THP can compensate for the postcursor ISI introduced by the asymmetric shaping filter, the penalty of the introduced ISI is better mitigated. By using the asymmetric-ISI pulse shaping filter and THP, we demonstrate 102 Gbaud PAM-4 transmission over 2 km in O-band below the 3.8×10^{-3} HD-FEC threshold using an 81-tap linear feedforward (FFE) equalizer at the receiver.

2. Pulse shaping filter with asymmetric ISI

The generation of the finite impulse response (FIR) pulse shaping filter with asymmetric ISI is based on the design and minimization of a cost function composed of cost terms that characterize the filter. Once the FIR filter taps are obtained, they can be saved into a lookup table. At two samples per symbol, an FIR pulse shaping filter can be formulated as $\mathbf{h} = [h_{-N} \ h_{-(N-1)} \ h_{-(N-2)} \ \dots \ h_{-2} \ h_{-1} \ 1 \ h_1 \ h_2 \ \dots \ h_{N-2} \ h_{N-1} \ h_N]$, where N is an even number. The cost function $F(\mathbf{h})$ is defined as $\lambda_1 C_{\text{PrecursorISI}} + \lambda_2 C_{\text{PostcursorISI}} + \lambda_3 C_{\text{OutofbandFreq}} + \lambda_4 C_{\text{HigherFreq}}$, where $C_{\text{PrecursorISI}}$, $C_{\text{PostcursorISI}}$, $C_{\text{OutofbandFreq}}$ and $C_{\text{HigherFreq}}$ represent the cost of the precursor ISI, the postcursor ISI, the out-of-band signal energy, and the in-band higher frequency signal energy, respectively. λ_k ($k = 1, 2, 3, 4$) is the coefficient assigned to the corresponding cost term to balance its weight in the total cost. In the cost function, the precursor ISI cost is defined as $\sum_{i=1}^{N/2} |h_{2*i-1}|$, while the postcursor ISI cost is defined as $\sum_{i=1}^{N/2} |h_{-(2*i-1)}|$. To obtain a bandlimited pulse shaping filter corresponding to a specific roll-off factor α , the energy of the frequency components beyond $(1+\alpha)/(2T)$ should be kept to zero, where T is the symbol duration. The out-of-band signal energy $C_{\text{OutofbandFreq}}$ is calculated as $\sum_{i \in \Omega} H_i * H_i^H = (Lh)^H Lh = h^H \text{Re}(L^H L) h$, where superscript H denotes conjugate transpose, H_i is the discrete frequency components of \mathbf{h} after discrete fourier transform (DFT), Ω is the set of indices corresponding to the out-of-band frequency components, and

L is expressed in (1) shown below with $W_k^n = \exp(\frac{-2\pi}{2N+1} kn)$. In a similar way, the cost term of the in-band higher frequency components $C_{higherFreq}$ is calculated as $\sum_{i \in \Phi} u_i H_i * (u_i H_i)^H = (uMh)^H (uMh) = h^T \text{Re}((uM)^H (uM)) h$, where Φ is the set of indices of the discrete in-band frequency components, M is expressed in (2), and u is the weight vector to add a higher cost to the higher frequency in-band components such that the signal power is constrained in lower frequency, resulting in increased Rx RF swing.

$$L = \begin{pmatrix} W_{N/2(1+\alpha)}^0 & W_{N/2(1+\alpha)}^1 & \cdots & W_{N/2(1+\alpha)}^{2N+1} \\ W_{N/2(1+\alpha)+1}^0 & W_{N/2(1+\alpha)+1}^1 & \cdots & W_{N/2(1+\alpha)+1}^{2N+1} \\ \vdots & \vdots & \ddots & \vdots \\ W_N^0 & W_N^1 & \cdots & W_N^{2N+1} \end{pmatrix} \quad (1), \quad M = \begin{pmatrix} W_0^0 & W_0^1 & \cdots & W_0^{2N+1} \\ W_1^0 & W_1^1 & \cdots & W_1^{2N+1} \\ \vdots & \vdots & \ddots & \vdots \\ W_{N/2(1+\alpha)-1}^0 & W_{N/2(1+\alpha)-1}^1 & \cdots & W_{N/2(1+\alpha)-1}^{2N+1} \end{pmatrix} \quad (2)$$

The cost function is minimized through the normal steepest gradient algorithm with an initial guess of h chosen as $[0 \dots 0 \ 0 \ 1 \ 0 \ 0 \dots 0]$, whose impulse response is depicted by the green dashed curve in Fig. 1(b).

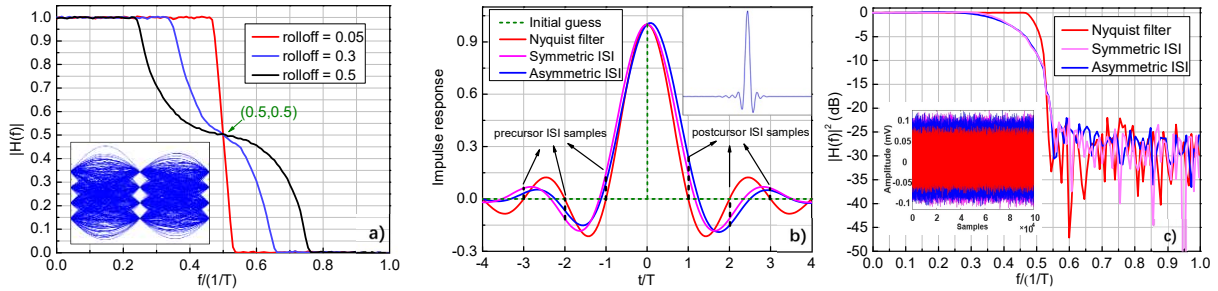


Fig. 1. (a) Converged Nyquist filters at different roll-off factors of 0.05, 0.3 and 0.5. (b) The impulse response of the converged pulse shaping filters at roll-off factor of 0.05. (c) Relative magnitude response of the pulse shaping filters at roll-off factor of 0.05.

We set N to 128 in our study and first converge Nyquist filters at different roll-off factors as shown in Fig. 1 (a) by assigning sufficiently large values to λ_1 and λ_2 . The satisfaction of the Nyquist zero ISI criterion is observed since the amplitude response is centrally symmetric about the point (0.5,0.5). This is also validated by the electrical eye diagram of a pulse shaped PAM-4 signal at a roll-off factor of 0.05 in the inset. Next, at a roll-off factor of 0.05, we increase λ_4 to raise the weight of $C_{higherFreq}$ and tune λ_1 and λ_2 accordingly to trade off the precursor and postcursor ISI for more constrained signal power in lower frequency. The impulse responses of the converged filters are shown in Fig. 1(b). Note that ISI mainly results from adjacent symbols, i.e. h_{-4}, h_{-2}, h_2, h_4 , since the amplitude of the impulse response decays rapidly with the time. It can be observed in the figure that the filter with asymmetric ISI is tuned to have stronger postcursor ISI than precursor ISI. The inset provides a rescaled view of the pulse shaping filter with asymmetric ISI. Figure 1(c) shows the relative magnitude response of the converged pulse shaping filters at a roll-off factor of 0.05. It is seen that the converged filters with ISI possess the same -15-dB bandwidth as the Nyquist filter by assigning a large weight to the cost term $C_{outofbandFreq}$. However, the filters with ISI roll off sharper, leading to more signal power constrained in lower frequency. This is also verified by the RF swing of the sampled waveforms of a 100 Gbaud PAM-4 signal in back to back (B2B) as shown in the inset, the color of which matches the curves in Fig. 1(c). We note in the inset that FIR filters with symmetric or asymmetric ISI increase the RF swing to a similar level compared to the Nyquist filter, but the filter with asymmetric ISI suits better for THP due to weaker precursor ISI.

3. Experimental set-up and results

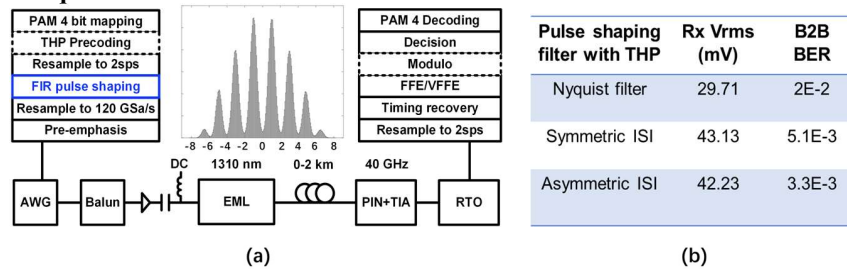


Fig 2. (a) Experimental set-up, (b) BER vs. pulse shaping filter with THP at 100 Gbaud at -3 dBm ROP in B2B.

Figure 2 (a) shows the experimental set-up. The transmitter has a 3-dB bandwidth of 14 GHz based on the pre-emphasis filter which flattens the transmitter response. The differential outputs of the AWG are fed to a balun and a driver amplifier (DA). The amplified RF signal drives an electro-absorption modulator (EAM) to modulate an integrated O-band optical source with a center wavelength of 1310 nm. After transmission, the RF signal is detected by a 40 GHz PIN+TIA and then sampled by a 63 GHz real-time oscilloscope (RTO). The Tx and Rx DSP block are shown in Fig. 2(a). Fig 2 (b) shows the root-mean-square (RMS) of the sampled 100 Gbaud PAM-4 signal and the corresponding BER at -3dBm received optical power (ROP) in B2B. The shaping filters with ISI significantly increase the RMS of the received RF signal, leading to lower BER. In particular, the pulse shaping filter with asymmetric ISI achieves almost an order of BER improvement relative to the Nyquist filter in B2B. It also outperforms pulse shaping filter with symmetric ISI due to less penalty induced by the precursor ISI. The inset in Fig. 2 (a) shows the seven-level amplitude histogram expanded from a 100 Gbaud PAM-4 signal shaped via an asymmetric-ISI filter.

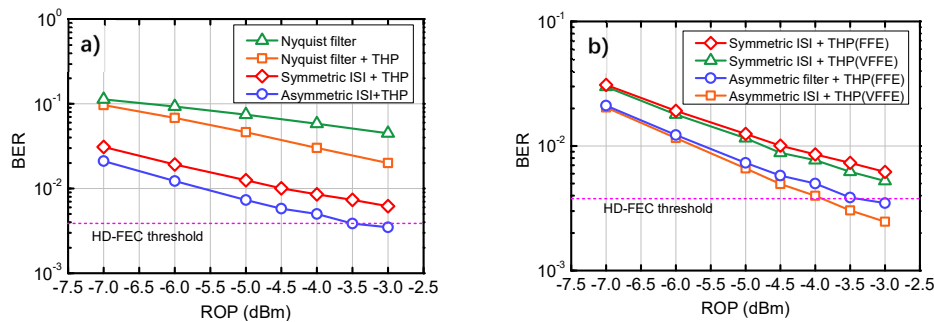


Fig 3. BER vs. ROP at 2km for (a) 102 Gbaud PAM-4, (b) Sensitivity improvement by VFFE at 102 Gbaud after 2 km

Figures 3(a) shows the BER vs. ROP for a 102 Gbaud PAM-4 signal transmitted over 2 km using an 81-tap FFE at the receiver. It can be observed that at the ROP of -3 dBm THP combined with FIR filter with asymmetric ISI is the only curve that goes below the HD-FEC BER threshold of 3.8×10^{-3} . The BER of the pulse shaping filter with symmetric ISI has a higher BER floor due to the introduced precursor ISI. When compared to the Nyquist filter shaped signal with THP, both filters with symmetric or asymmetric ISI achieve lower BER floor due to the enhanced RF swing at the receiver. We also note that Nyquist filter and THP outperforms Nyquist filter without THP since THP can mitigate the residual ISI in addition to the ISI pre-compensated by the pre-emphasis filter at the transmitter.

Figure 3(b) shows the sensitivity improvement by use of a Volterra FFE (81,9,5) for a 102 Gbaud PAM-4 signal transmitted over 2 km. In the figure, a 0.4 dB sensitivity gain is observed at the HD-FEC threshold for a precoded PAM-4 signal shaped via an FIR filter with asymmetric ISI at the cost of additional 45 second-order taps and 35 third order taps. This means that for 102 Gbaud PAM-4 transmission using this set-up, the RF swing is relatively small such that the nonlinearity resulting from the EAM and DA is marginal. This is also verified by the amplitude histogram shown in Fig. 2 (a), where the symbols are almost evenly distributed after FFE.

4. Conclusion

In this paper, we propose to increase the receiver RF swing in a high baud PAM-4 system by use of a pulse shaping filter with asymmetric ISI and THP. The filter is obtained based on a cost-function that allows the flexible tuning of the cost terms such that a balance can also be struck between the introduced ISI penalty and the receiver RF swing. By applying this filter with asymmetric ISI and THP in a 1310 nm O-band system, we demonstrate 102 Gbaud transmission over 2 km below the 3.8×10^{-3} HD-FEC BER threshold.

5. Reference

- [1] 802.3bs-2017 - IEEE Standard for Ethernet. [Online]. Available: <https://ieeexplore.ieee.org/document/8207825/>. [Accessed Oct. 9, 2019].
- [2] T. Wettlin, et al., "Beyond 200 Gb/s PAM4 Transmission using Tomlinson-Harashima Precoding," Proc. ECOC 2019, Paper Tu2B.6
- [3] Q. Hu, et al., "84 GBd Faster-Than-Nyquist PAM-4 Transmission Using Only Linear Equalizer at Receiver," Proc. OFC 2019, paper W4I-2.
- [4] M. Xiang, et al., "Single-Lane 145 Gbit/s IM/DD Transmission with Faster-Than-Nyquist PAM4 Signaling," IEEE Photon. Technol. Lett., **30**, pp. 1238-1241 (2018).
- [5] Z. Xing, et al., "600G PAM4 Transmission Using a 4-Lambda CWDM TOSA Based on Controlled-ISI Pulse Shaping and Tomlinson-Harashima Precoding," Proc. ECOC 2019, paper Tu3D.1.